Supporting Information

Tailoring Thermoplastic In-Plane Nanopore Size by Thermal Fusion Bonding for the Analysis of Single Molecules

Uditha S. Athapattu,[1,2‡] Chathurika Rathnayaka,[1,2‡] Swarnagowri Vaidyanathan,[2,3‡] Sachindra S. T. Gamage,[1,2‡] Junseo Choi,[2,4] Ramin Riahipour,[2,4] Anishkumar Manoharan,[1,2] Adam R. Hall,[5*] Sunggook Park,[2,4*] and Steven A. Soper[1,2,3,6,7*]

[1]Department of Chemistry, The University of Kansas, Lawrence, KS 66045

[2]Center of BioModular Multiscale Systems for Precision Medicine

[3]Bioengineering Program, The University of Kansas, Lawrence, KS 66045

[4]Mechanical & Industrial Engineering Department, Louisiana State University, Baton Rouge, LA 70803

[5]Virginia Tech-Wake Forest University School of Biomedical Engineering and Sciences and Comprehensive Cancer Center, Wake Forest School of Medicine, Winston-Salem, NC 27101

[6]Department of Mechanical Engineering, The University of Kansas, Lawrence, KS 66045

[7]KU Cancer Center, University of Kansas Medical Center, Kansas City, KS 66160

[‡]These authors contributed equally to this work.

[*]Authors to whom correspondence should be addressed.

Corresponding author's email; ssoper@ku.edu

Reagents and materials. Chemicals and other materials were obtained from the following sources and used without further purification: S1813 photoresist (MicroChemicals, Germany); MF319 developer (MicroChemicals); potassium hydroxide (KOH) pellets (Fisher Scientific, Waltham, MA); isopropyl alcohol (IPA; Sigma-Aldrich, St. Louis, MO); hydrofluoric acid (HF, Sigma-Aldrich); Tri(propylene glycol) diacrylate (TPGDA, Sigma-Aldrich); Trimethylolpropane triacrylate (TMPTA, Sigma-Aldrich); 2,2-Dimethoxy-2-phenylacetophenone (photoinitiator, Sigma-Aldrich); NOA72 (Norland Products, Neuchâtel, Switzerland); Si wafers (P/B, resistivity 5-10 Ωcm, orientation of (100), and 525 ± 25 μm thickness, WaferPro, Santa Clara, CA); polyethylene terephthalate (PET) with 250 μm thickness (Goodfellow, Coraopolis, PA). Silicon (Si) 〈100〉 wafers were purchased from University Wafers (Boston, MA). PMMA was received from ePlastics (San Diego, CA). COC (Type 8007) was purchased from TOPAS Advanced Polymers (Florence, KY). COP sheets were obtained from STRATEC SE (Birkenfeld, Germany). UV curable polyurethane resin was purchased from Chansang Co. Guanosine 5'-monophosphate disodium salt was obtained from Sigma-Aldrich. Molecular biology grade water was secured from Thermo Fisher (Waltham, MA). SYTO82 dye was from Life Technologies (Eugene, OR, USA).

Device fabrication and assembly. Si wafers with a 100 nm thick silicon nitride (Si_3N_4) layer on each side were used for fabricating a Si master mold. Microchannels were fabricated using a combination of photolithography and wet-chemical etching. To accomplish this, a 1.3 μm thick S1813 photoresist layer was first spin-coated at 4,000 rpm for 60 s on a Si wafer and then baked at 115°C for 60 s. Photolithography was performed using a designed photomask in a UV exposure station (Quintel) in a class 100 cleanroom. UV exposure was conducted at 130-140 mJ/cm^2 with post-exposure baking at 95°C for 60 s. Then, the wafer was developed with a MF319 developer for 90 s, followed by washing with deionized water. The exposed Si_3N_4 layer was etched to open a window using an ICP-DRIE system (Plasmalab System 100, Oxford Instruments, Abingdon, UK). Subsequently, the wafer was transferred to a 40 wt% KOH solution with IPA (5 % v/v) at 70°C. The KOH solution was prepared by dissolving KOH pellets in deionized water. After 25 min etching to form 10 μm deep microchannels, the wafer was removed from the etchant, rinsed in water, and dried with N_2 gas. Prior to FIB milling, the Si_3N_4 layer was completely removed using a dilute HF solution. The nanochannel flight tube combined with in-plane nanopores was fabricated using FIB milling (Quanta 3D Dual Beam system, FEI, Hillsboro, OR). The milling was performed at a beam voltage and current of 30 kV and 10 pA, respectively, in a bitmap mode.

The Si master mold was used to produce a resin stamp by using a UV resin solution (70 wt% TPGDA, 28 wt% TMPTA, and 2 wt% photoinitiator). Drops of the UV-resin were dispensed against the Si master mold. A flexible PET sheet coated with an adhesive layer (NOA72) was then slightly

pressed against the liquid drop and used as a backbone for the resin stamp. Residual resin solution and air bubbles were gently squeezed out. During the curing process, the sample was exposed to flash-type UV light (250-400 nm) for 20 s at an intensity of ~1.8 W/cm^2 by using a nanoimprinter (Eitre6, Obducat, Lund, Sweden). After UV-curing, the molded UV-resin/PET backbone was demolded from the Si master.

Nanopore devices were imprinted into a plastic substrate using nanoimprint lithography ,NIL (Nanonex 2500, Monmouth Junction, NJ).[1] The optimized imprinting conditions were 145°C, 300 psi, and 5 min for PMMA nanofluidic devices, and 130°C, 300 psi, and 5 min for COP devices. Imprinted nanofluidic devices were then characterized using scanning electron microscope (SEM), and atomic force microscopy (AFM).

The imprinted nanopore devices were then sealed using a COC 8007 cover plate. Thermal fusion bonding with NIL was used for sealing nanopore devices. Bonding of PMMA/COC devices was done following the method described by Uba *et al*.[2] following 1 min O_2 plasma treatment for both the substrate and cover plate at 50 W.

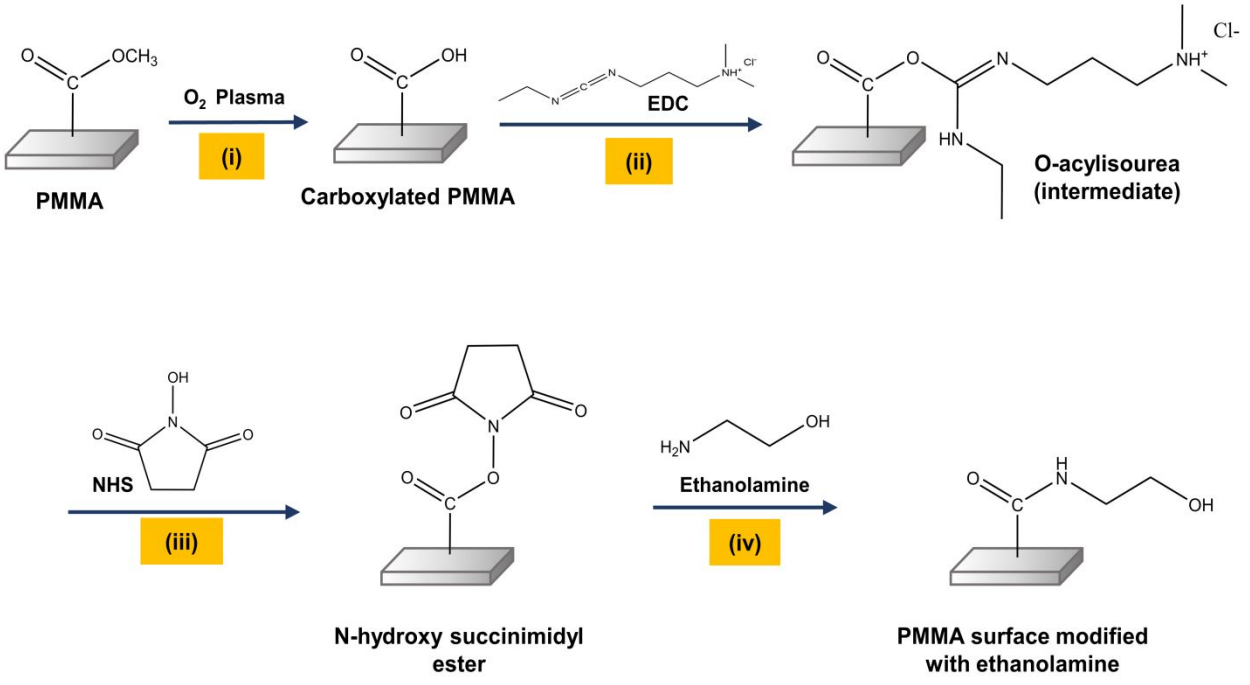

Figure S1. Protocol for the surface modification of PMMA (or COC) devices by: **(i)** Generation of surface confined carboxyl groups using O_2 plasma activation; **(ii)** O-acylisourea intermediate by reaction with EDC; **(iii)** N-hydroxy succinimidyl ester generation with NHS; and **(iv)** surface hydroxyl groups by treatment with ethanolamine

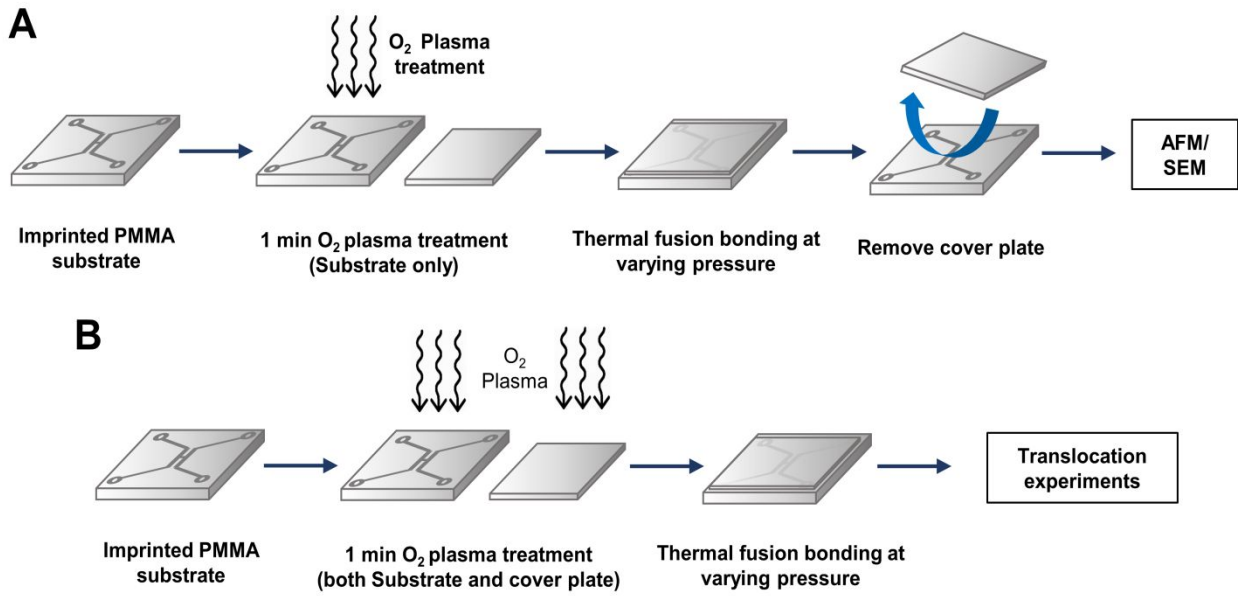

Figure S2. **(A)** Schematic representation of experimental procedure for determining depth and width of dual in-plane nanopores. **(B)** Schematic representation of device assembly for translocation studies.

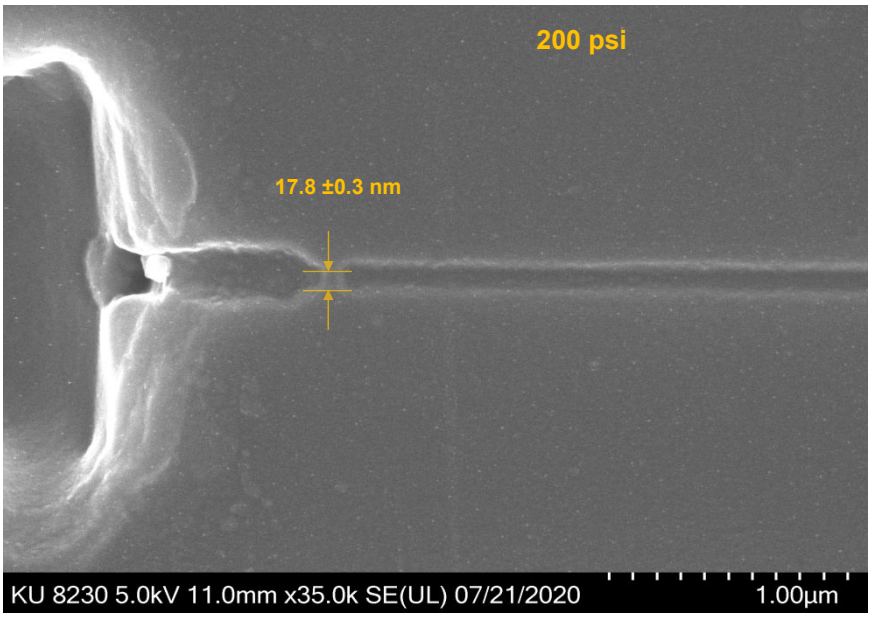

Figure S3. SEM image of PMMA device at 200 psi bonding pressure. A 2 nm thin conductive Iridium layer was sputter coated onto the PMMA device using an EMS 150ES sputter coater before SEM Imaging.

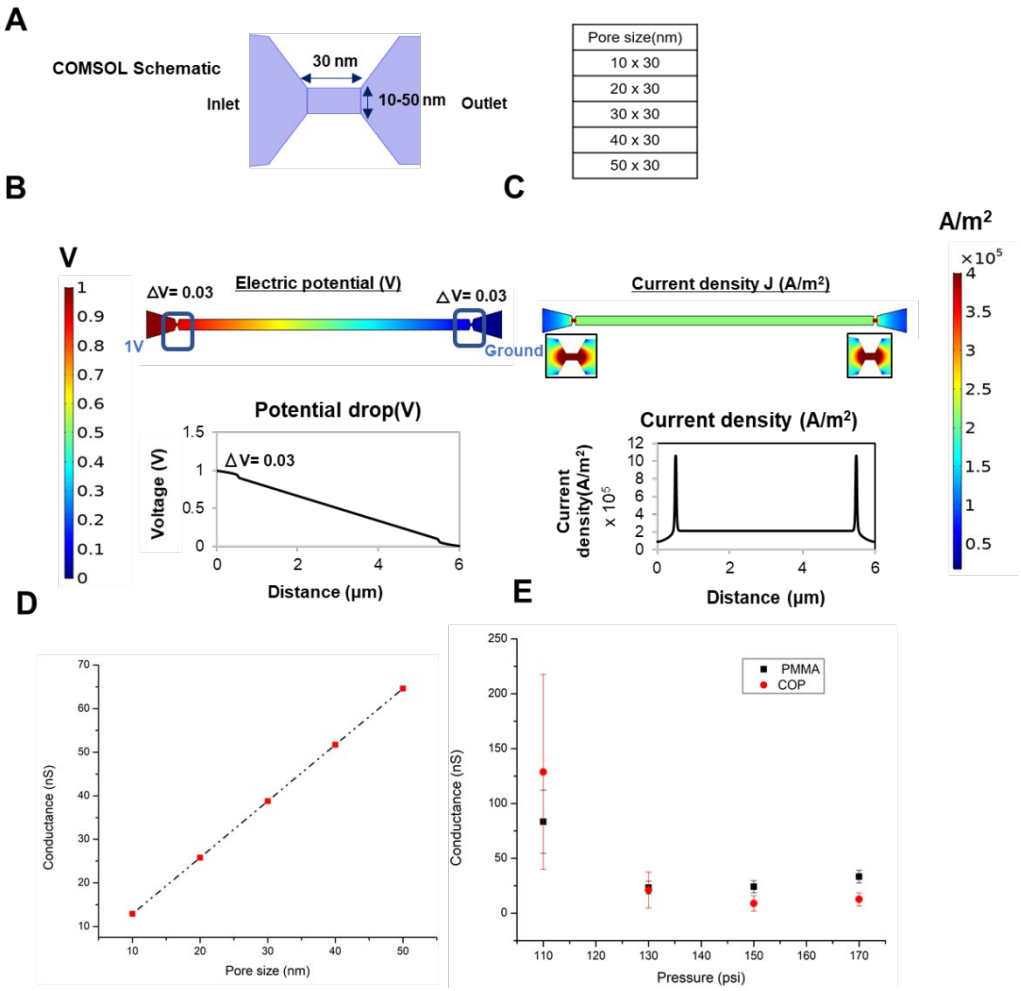

Figure S4. Simulated and experimental analysis of the electrical behavior of the dual in-plane nanopores connected by a 5 μm length flight tube at different bonding pressures. **(A)** The 2D design of the dual in-plane nanopores used for COMSOL simulations. The pore and intervening 5 μm long nanochannel were assumed to be cylindrical. In order to understand if a change of in-plane nanopore diameter would cause an increase in conductance, the pore diameter was varied from 10-50 nm while the length was kept constant at 30 nm. **(B)** The electric potential data from COMSOL simulations shows that the majority of the potential drop appears across the two nanopores and the nanochannel implying that the overall conductance is contributed by the two nanopores and the nanochannel. **(C)** The current density was plotted from which the current and the subsequent conductance was calculated (I/V). **(D)** Conductance (nS) calculated from COMSOL for varying pore widths in 1 M KCl. There was a linear increase in conductance with increasing pore width. **(E)** Variation of measured conductance through the dual in plane nanopore PMMA and COP devices at different bonding conditions using an electrolyte of 1 M KCl (n ≥3). There was a decrease in conductance with increase in bonding pressure, but with no statistical differences at pressures above 130 psi ($p > 0.05$). The conductance results agree with the pore size determined using AFM and SEM and were also correlated to the COMSOL results. The y-axis scales of graphs for (**D**) and (**E**) are adjusted according to their corresponding x-axis and hence the range might be different.

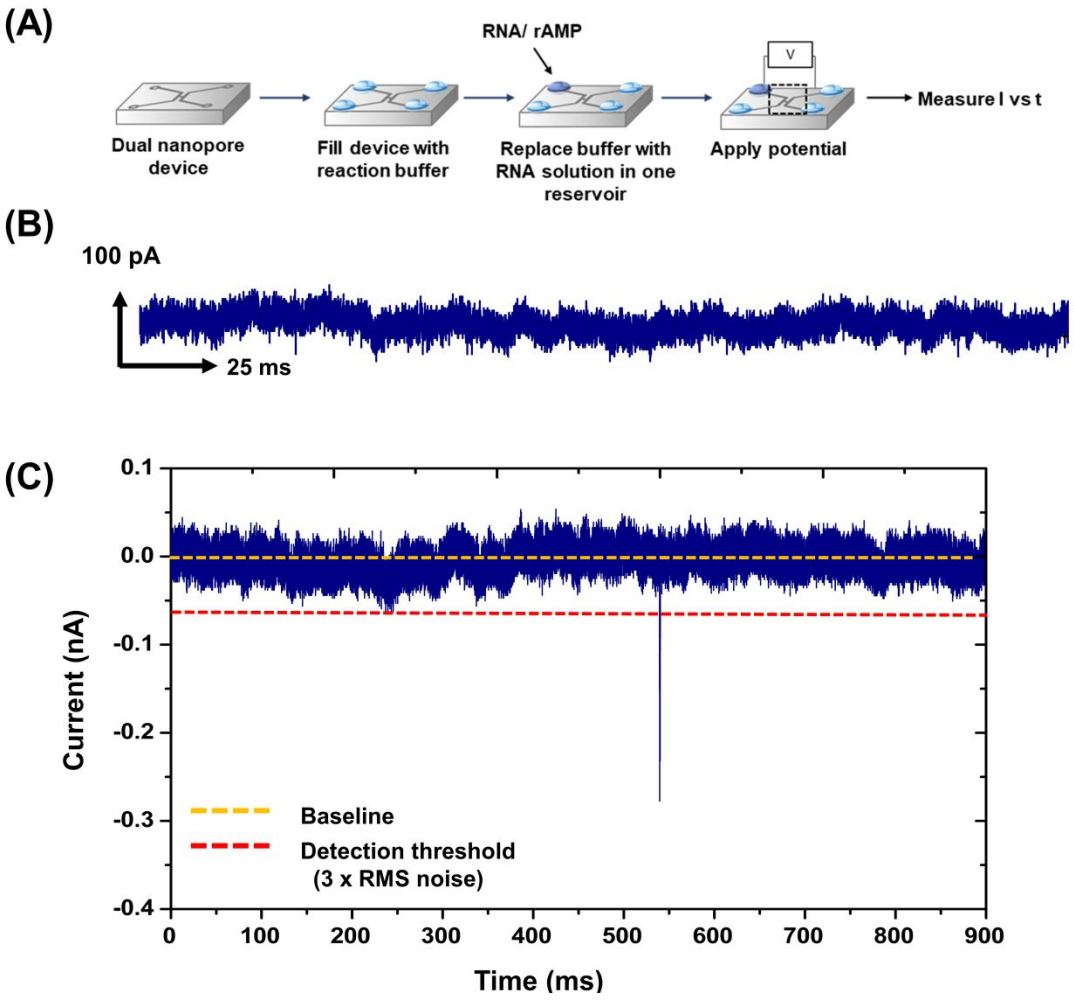

Figure S5. Biomolecule translocation through dual in-plane nanopores under an applied electric field. **(A)** Schematic representation of the reaction procedure and subsequent ssRNA (60 nt) translocation experiments. In this case, the reaction consisted of EDC/NHS and ethanolamine, which was used to react with the surface carboxyl groups following O_2 plasma activation of the PMMA surface. **(B)** A 250 ms current transient trace of the open pore (baseline) current. **(C)** A 900 ms current trace obtained after the introduction of a 60 nt long RNAs in an O_2 plasma treated PMMA dual in-plane nanopore device. The open pore current was subtracted from this trace.

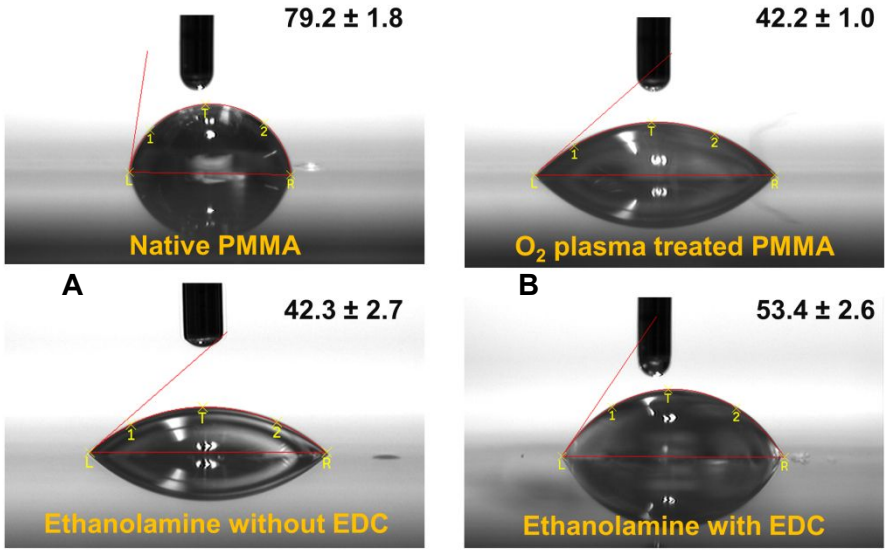

Figure S6. Sessile water contact angle measurements of a native PMMA surface (**A**), followed by O_2 plasma treatment to generate surface carboxyl groups (**B,**) reaction with ethanolamine in the presence (**C**) and absence (**D**) of EDC/NHS coupling chemistry.

Sessile drop water contact angle measurements. The hydrophilicity/hydrophobicity of native, O_2 plasma modified and ethanolamine modified PMMA surfaces were determined by sessile drop water contact-angle measurements using a VCA Optima instrument (AST Products). PMMA sheets (1.5 mm thick) were cut into 1.5 cm $\times$ 1.5 cm sections and 2.0 µL of a nanopure water drop (pH 7.5) was dispensed onto the surface followed by capturing images and analyzing the sessile contact angle using the software provided by the manufacturer. The measurements reported were the mean $\pm$ the standard deviation of five drops at separate positions of the PMMA substrate. Results for these measurements are shown in Figure S3, which show contact angles for native PMMA, PMMA treated with an O_2 plasma, and plasma treated with ethanolamine in the absence and presence of EDC/NHS coupling chemistry.

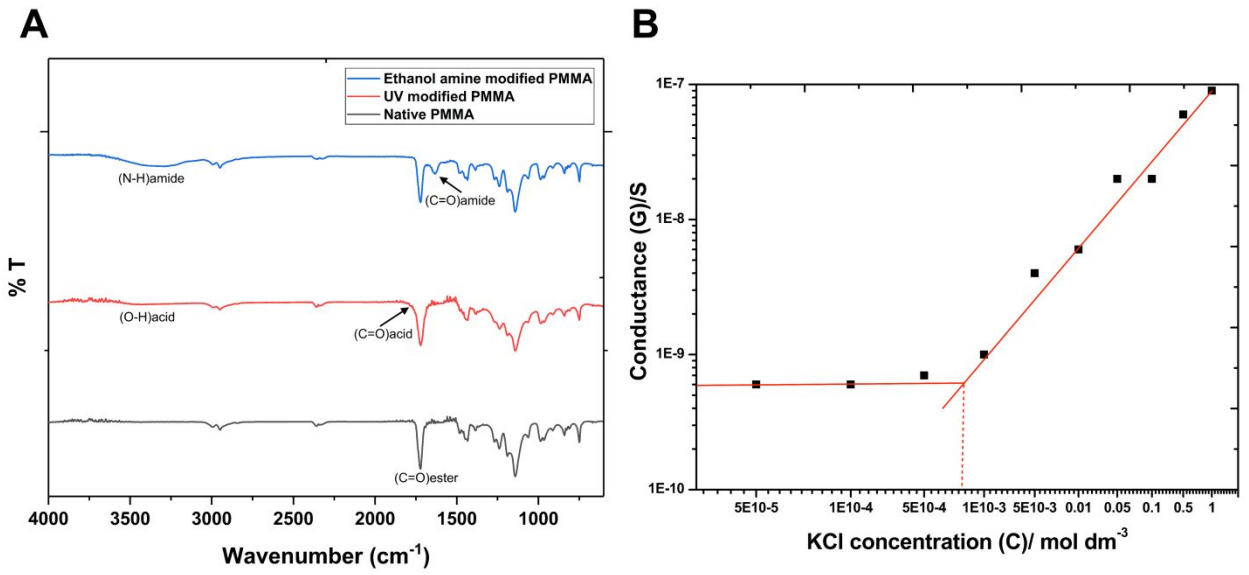

C

	EOF (cm^2/ V s)	Surface charge (mC/ m^2)	Zeta potential (mV)
ETA modified PMMA	3.63 (±0.10) x 10^{-5}	-3.8	-5.2
O_2 plasma modified PMMA	4.10 (±0.10) x 10^{-4}	-40.1	-59

Figure S7. Surface characterization of ethanolamine (ETA) modified PMMA surfaces. **(A)** ATR-FTIR spectra of native, UV activated, and ethanolamine modified PMMA. **(B)** Conductance versus KCl concentration obtained from ethanolamine modified PMMA devices consisting an array of four nanochannels (each channel was 100 nm wide, 100 nm deep, and 107 μm long). Each data point represents a mean of five measurements with the scatter in the data <5-8% of the average. The calculated effective surface charge density from the graph was -3.8 mC/m^2. **(C)** Measured EOF values as well as surface charge density and zeta potential for ethanolamine modified PMMA nanochannel devices investigated at pH 7.8. The EOF and zeta potential for O_2 plasma modified PMMA were reproduced from Amarasekara *et al*.[3] The surface charge density for plasma modified nanochannel devices was reproduced from Uba *et al*.[4]

ATR-FTIR characterization of ethanolamine modified surfaces. To examine the molecular nature of the modified and unmodified thermoplastic surfaces with ethanolamine, ATR-FTIR experiments were performed. As noted in literature, ATR-FTIR has penetration depths of 0.5-2 μm into the bulk material and therefore, thermoplastics were UV/O_3 activated for 15 min at 22 mW cm^{-2} power prior to ethanolamine modification.[5] The surfaces activated with UV/O_3 observed sufficient ATR-FTIR signal (see Figure S7A) as activation occurs into the depth of the thermoplastics whereas, O_2 plasma activation occurs only within first few monolayers. An ATR-FTIR spectrum of native PMMA with the characteristic peaks between 4000 and 500 cm^{-1} is shown in Figure S7A. The most prominent band was ν(C=O) at 1724 cm^{-1} assigned to the methacrylate ester stretch. The peaks at 1270, 1240 cm^{-1} and 1195, 1150 cm^{-1} could be assigned to ν(C-O) and ν(C-O-C) stretching of an ester. After UV/O_3 activation, there was the appearance of a band at 3441 cm^{-1} and 1737 cm^{-1}, which could be assigned to the ν(O-H) and ν(C=O) of a carboxylic

acid group.[4, 6] Upon treatment with ethanolamine bands at 3396 cm^{-1} and 1635 cm^{-1} corresponded to the v(N-H) stretch of a primary amine and v(C=O) of an amide.

Surface Charge. We used electrical conductance measurements across ethanolamine modified nanochannel device filled with different KCl concentrations to work out the surface charge density. The average conductance was plotted against the electrolyte concentration in a log-log plot (see Figure S7B) and the surface charge (σ_s) density was deduced by fitting the conductance plot according to;[4]

$$G_T = 10^3(\mu_{K^+} + \mu_{Cl^-})cN_Ae.\frac{nwh}{L} + 2\mu_{opp}\sigma_s n\frac{(w+h)}{L} \quad (1)$$

where G_T is the total measured conductance in the nanochannel, μ_{K^+} and μ_{Cl^-} are ion mobilities of K^+ and Cl^- ions, respectively (μ_{K^+} = 7.619 × 10-8 $m^2\ V^{-1}\ s^{-1}$ and μ_{Cl^-}=7.912 × 10^{-8} $m^2\ V^{-1}\ s^{-1}$), c is the electrolyte concentration in mol L^{-1}, N_A is Avogadro's number, e is the electron charge, n is the number of nanochannels in the device, w, h, and L are width, height and length of the nanochannel respectively, and $\mu_{opp} \approx \mu_{K^+}$ for the deprotonated carboxyl surface (see Figure S7B).

It is reported that carboxylic acid groups are generated on PMMA and COC upon UV/O_3 activation[7] or O_2 plasma treatment.[8, 9] After ethanolamine modification of O_2 plasma treated devices, the surface is dominated by hydroxyl groups. When ethanolamine modified surfaces are in contact with an electrolyte solution at pH 7.8, ~99.9% of the hydroxyl groups (pK_a = 16.0) would be protonated and ~99.9% of the carboxyl groups (pK_a = 4.66) would be deprotonated.[10] Therefore, these deprotonated carboxylic acid moieties are responsible for generating a surface charge density. The transition concentration, c_t used to calculate σ_s was 0.78 mM for ethanolamine modified surface. For ethanolamine modified PMMA nanochannels, we obtained σ_s ~ -3.8 mC/m^2, which was ~10-fold less than -40.5 mC/m^{-2} reported by Uba *et al.* for O_2 plasma modified nanochannels.[4]

Electroosmotic flow. the EOF of ethanolamine modified nanochannel device was measured using the current monitoring method.[11] The EOF can be described by $\mu_{eof} = \upsilon_{eof}/E$, where υ_{eof} is electroosmotic flow velocity and E is the field strength. As noted above, plasma activated PMMA surfaces are negatively charged due to deprotonation of carboxylic acid groups and ethanolamine modified PMMA surfaces are uncharged at pH 7.8. The EOF for ethanolamine modified PMMA nanochannel device was 3.63 × 10^{-5} $cm^2/\ V\ s$ (see Figure S7C), which was ~9-fold less than 4.1 × 10^{-4} $cm^2/\ V\ s$ reported by Amarasekara *et al.* for O_2 plasma modified PMMA nanochannel device.[3] The zeta potential, ζ was computed using equation (2). At low electric double layer

thicknesses ($\lambda_D \approx 0.8$ nm for 1X NE buffer 3) μ_{eof} can be represented by Helmholtz-Smoluchowski equation;

$$\mu_{eof} = \frac{\varepsilon_0 \varepsilon_r \zeta}{\eta_0} \quad (2)$$

where ε_0, ε_r are the permittivity of vacuum, and the relative permittivity of the buffer (80.1), respectively, ζ is the zeta potential and η_0 is the bulk solvent viscosity (8.9×10^{-4} Pa/s).[2] The computed zeta potential for ethanolamine modified PMMA device was -5.2 mV and it was ~11-fold less compared to O_2 plasma modified device.[3] The surface charge density, EOF and the zeta potential values further supports the successful modification of PMMA surfaces with ethanolamine.

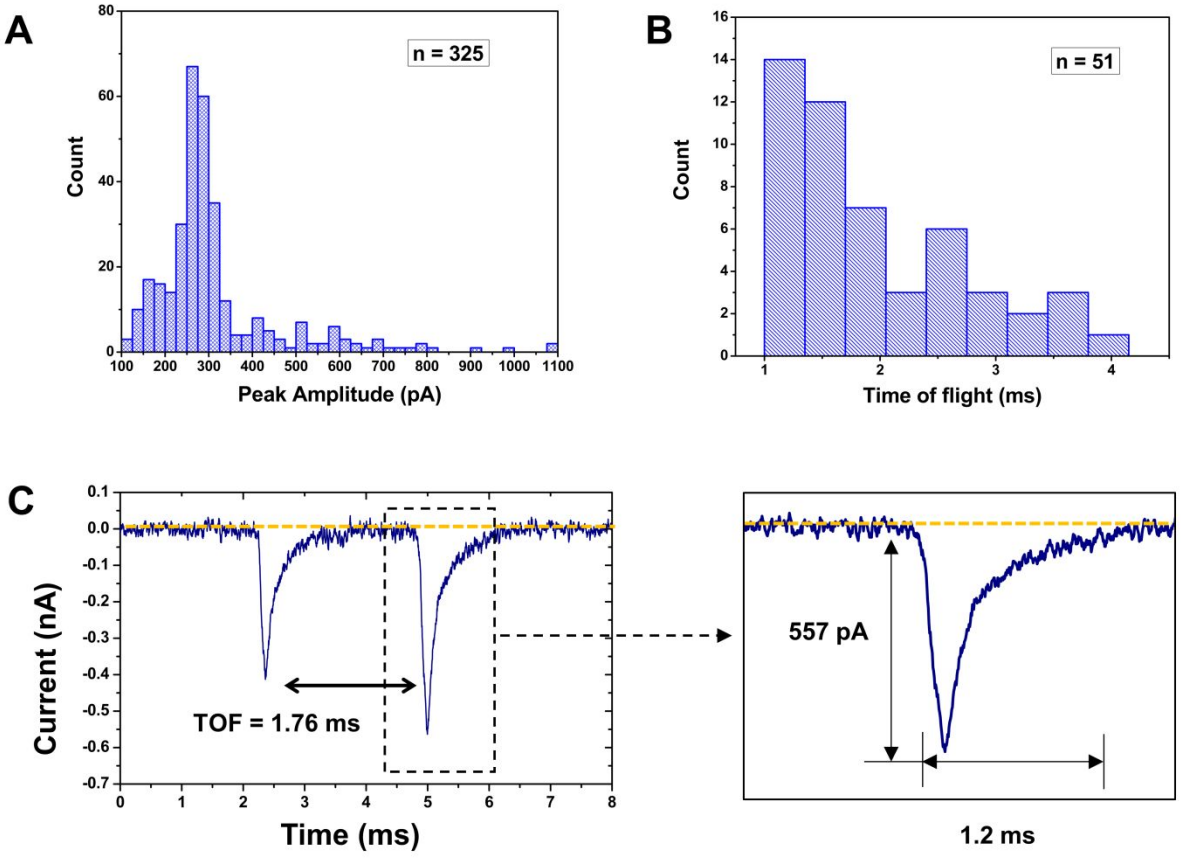

Figure S8. Translocation of 60 nt ssRNA through dual in-plane nanopore devices bonded at 170 psi. (**A**) Histogram of the current transient amplitudes for the 60 nt ssRNA. The current transient amplitudes ranged between 0.10 – 0.8 nA with an average of 311.75 ±137.49 pA (n = 325). **(B)** Histogram of the time-of-flight (TOF) values obtained for the 60 nt ssRNA. The TOF ranged between 1 – 4 ms with an average of 2.09 ±0.97 ms (n = 51). **(C)** An example peak pair as determined based on the peak pair selection criteria.

References

1. Amarasekara, C. A.; Rathnayaka, C.; Athapattu, U. S.; Zhang, L.; Choi, J.; Park, S.; Nagel, A. C.; Soper, S. A., Electrokinetic identification of ribonucleotide monophosphates (rNMPs) using thermoplastic nanochannels. *Journal of Chromatography A* **2021,** *1638*, 461892.

2. Uba, F. I.; Hu, B.; Weerakoon-Ratnayake, K.; Oliver-Calixte, N.; Soper, S. A., High process yield rates of thermoplastic nanofluidic devices using a hybrid thermal assembly technique. *Lab on a Chip* **2015,** *15* (4), 1038-1049.

3. Amarasekara, C. A.; Athapattu, U. S.; Rathnayaka, C.; Choi, J.; Park, S.; Soper, S. A., Open-tubular nanoelectrochromatography (OT-NEC): gel-free separation of single stranded DNAs (ssDNAs) in thermoplastic nanochannels. *Electrophoresis* **2020,** *41* (18-19), 1627-1640.

4. Uba, F. I.; Pullagurla, S. R.; Sirasunthorn, N.; Wu, J.; Park, S.; Chantiwas, R.; Cho, Y.-K.; Shin, H.; Soper, S. A., Surface charge, electroosmotic flow and DNA extension in chemically modified thermoplastic nanoslits and nanochannels. *Analyst* **2015,** *140* (1), 113-126.

5. Mirabella, F. M., *Internal reflection spectroscopy: theory and applications*. CRC Press: 1992; Vol. 15.

6. Henry, A. C.; Tutt, T. J.; Galloway, M.; Davidson, Y. Y.; McWhorter, C. S.; Soper, S. A.; McCarley, R. L., Surface modification of poly (methyl methacrylate) used in the fabrication of microanalytical devices. *Analytical chemistry* **2000,** *72* (21), 5331-5337.

7. Jackson, J. M.; Witek, M. A.; Hupert, M. L.; Brady, C.; Pullagurla, S.; Kamande, J.; Aufforth, R. D.; Tignanelli, C. J.; Torphy, R. J.; Yeh, J. J., UV activation of polymeric high aspect ratio microstructures: ramifications in antibody surface loading for circulating tumor cell selection. *Lab on a Chip* **2014,** *14* (1), 106-117.

8. Vesel, A.; Mozetic, M., Surface modification and ageing of PMMA polymer by oxygen plasma treatment. *Vacuum* **2012,** *86* (6), 634-637.

9. Roy, S.; Yue, C.; Lam, Y.; Wang, Z.; Hu, H., Surface analysis, hydrophilic enhancement, ageing behavior and flow in plasma modified cyclic olefin copolymer (COC)-based microfluidic devices. *Sensors and Actuators B: Chemical* **2010,** *150* (2), 537-549.

10. Meisenberg, G.; Simmons, W. H., *Principles of medical biochemistry*. Mosby Elsevier: 2006.

11. Huang, X.; Gordon, M. J.; Zare, R. N., Current-monitoring method for measuring the electroosmotic flow rate in capillary zone electrophoresis. *Analytical chemistry* **1988,** *60* (17), 1837-1838.